

Published in final edited form as:

*Nat Biotechnol.* 2009 April ; 27(4): . doi:10.1038/nbt.1534.

## A molecular barcoded yeast ORF library enables mode-of-action analysis of bioactive compounds

Cheuk Hei Ho<sup>#1,2</sup>, Leslie Magtanong<sup>#1,2</sup>, Sarah L Barker<sup>#1,2</sup>, David Gresham<sup>3</sup>, Shinichi Nishimura<sup>4,5</sup>, Paramasivam Natarajan<sup>6</sup>, Judice L Y Koh<sup>1,2</sup>, Justin Porter<sup>7</sup>, Christopher A Gray<sup>7</sup>, Raymond J Andersen<sup>7</sup>, Guri Giaever<sup>1,2,8</sup>, Corey Nislow<sup>1,2</sup>, Brenda Andrews<sup>1,2</sup>, David Botstein<sup>3</sup>, Todd R Graham<sup>6</sup>, Minoru Yoshida<sup>4</sup>, and Charles Boone<sup>1,2,4</sup>

<sup>1</sup>Department of Molecular Genetics, University of Toronto, Toronto, Ontario, Canada.

<sup>2</sup>Banting and Best Department of Medical Research, Terrence Donnelly Centre for Cellular and Biomolecular Research, University of Toronto, Toronto, Ontario, Canada.

<sup>3</sup>Lewis-Sigler Institute for Integrative Genomics, Princeton University, Princeton, New Jersey, USA.

<sup>4</sup>Chemical Genetics Laboratory/Chemical Genomics Research Group, RIKEN Advanced Science Institute, Saitama, Japan.

<sup>5</sup>Graduate School of Pharmaceutical Sciences, Kyoto University, Kyoto, Japan.

<sup>6</sup>Department of Biological Sciences, Vanderbilt University, Nashville, Tennessee, USA.

<sup>7</sup>Department of Chemistry, Earth & Ocean Sciences, University of British Columbia, Vancouver, British Columbia, Canada.

<sup>8</sup>Department of Pharmaceutical Sciences, University of Toronto, Toronto, Ontario, Canada.

# These authors contributed equally to this work.

### Abstract

We present a yeast chemical-genomics approach designed to identify genes that when mutated confer drug resistance, thereby providing insight about the modes of action of compounds. We developed a molecular barcoded yeast open reading frame (MoBY-ORF) library in which each

© 2009 Nature America, Inc. All rights reserved.

Correspondence should be addressed to C.B. (charlie.boone@utoronto.ca) or M.Y. (yoshidam@riken.jp).

Note: Supplementary information is available on the Nature Biotechnology website.

**AUTHOR CONTRIBUTIONS** C.H.H. was involved in MoBY-ORF construction, carried out experiments, data analysis and interpretation of cloning drug-resistant mutants, carried out the genetic and cell biological experiments to characterize the MOAs of theopalauamide and stichloroside and wrote the manuscript; L.M. was involved in MoBY-ORF construction and wrote the manuscript; S.L.B. was involved in MoBY-ORF construction, sequencing and functional studies of the MoBY-ORF library, and wrote the manuscript; D.G. carried out all the experiments and data analysis of the YTM experiments, and wrote the manuscript; S.N. carried out all the experiments and data analysis of the *in vitro* ergosterol binding experiment, prepared fluorescently-labeled theonellamide A, and wrote the manuscript; P.N. carried out experiments and data analysis of the liposome leakage experiments, and wrote the manuscript; J.L.Y.K. provided computational support for MoBY-ORF validation, database construction and sequencing analysis; J.P. purified theopalauamide and stichloroside; C.A.G. purified theopalauamide and stichloroside; R.J.A. purified theopalauamide and stichloroside, and edited the manuscript; G.G. provided data analysis of cloning drug-resistant mutants with MoBY-ORF complementation using barcode microarray, and edited the manuscript. C.N. provided data analysis of cloning drug-resistant mutants with MoBY-ORF complementation using barcode microarray, and edited the manuscript; B.A. edited the manuscript; D.B. was involved in YTM analysis and edited manuscript; T.R.G. provided data analysis of all of the liposome leakage experiments, and wrote the manuscript; M.Y. provided data analysis and interpretation of the theopalauamide and theonellamide results, and wrote the manuscript; C.B. conceived and planned the construction of the MoBY-ORF library, provided data analysis and interpretation of the results, and wrote the manuscript.

gene, controlled by its native promoter and terminator, is cloned into a centromere-based vector along with two unique oligonucleotide barcodes. The MoBY-ORF resource has numerous genetic and chemical-genetic applications, but here we focus on cloning wild-type versions of mutant drug-resistance genes using a complementation strategy and on simultaneously assaying the fitness of all transformants with barcode microarrays. The complementation cloning was validated by mutation detection using whole-genome yeast tiling microarrays, which identified unique polymorphisms associated with a drug-resistant mutant. We used the MoBY-ORF library to identify the genetic basis of several drug-resistant mutants and in this analysis discovered a new class of sterol-binding compounds.

---

Identifying the cellular targets of a chemical compound is a critical challenge in drug discovery. Because many medicinally important drugs target fundamental, conserved biological processes, chemical-genomic approaches in the budding yeast *Saccharomyces cerevisiae* represent a useful means for elucidating the modes of action (MOAs) of a broad spectrum of compounds. These approaches include drug-induced haploinsufficiency<sup>1</sup>, dosage-dependent suppressor screens<sup>2-5</sup> and chemical-genetic profiling of single-gene deletion mutants<sup>6-9</sup>. Despite the impressive potential of these assays, however, each has limitations. Haploinsufficiency-based approaches are unlikely to identify a drug target that is the product of an enzyme rather than the enzyme itself. Dosage-dependent suppressor screens often pick up spurious genes associated with off-target effects or physiological responses to the drug, which confound efforts to identify the primary drug target. The approaches based upon clustering of chemical-genetic profiles are somewhat difficult to implement because they depend upon the assembly of a relatively large compendium of reference profiles. Thus, further development of new chemical-genomics resources and methodologies remains an important goal.

An alternative strategy uses drug-resistant mutations to identify genes encoding components of the targeted pathway<sup>9-15</sup>. For example, mutations in tumor cells to the gene encoding  $\beta$ -tubulin have been shown to confer resistance to the chemotherapeutic agent taxol<sup>16</sup>, and mutations in the yeast *FKSI*, which encodes a cell wall 1,3- $\beta$ -D-glucan synthase, have been associated with resistance to caspofungin, an antifungal drug that inhibits this enzyme directly<sup>10,17</sup>. Because many drug-resistant mutations are recessive, cloning by complementation (that is, by introducing a wild-type copy of the gene to complement the drug-resistant phenotype) is often feasible<sup>9-11,15</sup>. Typically, in these assays, the drug-resistant mutant strain is transformed with a library of random fragments of the yeast genome and each of the resulting transformants is screened for drug sensitivity. Although effective, this procedure is labor intensive and often requires prohibitive amounts of the drug, making the approach generally unsuitable for large-scale analysis when only a limited amount of the compound is available.

Here we present a comprehensive strategy for identifying drug-resistant mutations in yeast. We constructed a MoBY-ORF library that enables the effects of introducing individual genes into a mutant strain to be efficiently assayed. The DNA barcodes allow simultaneous measurements using microarrays of the fitness of cells in heterogeneous populations transformed with the entire library, thereby minimizing the amount of the drug required for the complementation assay. We attempted to validate the complementation cloning by using whole-genome yeast tiling microarray (YTM) to identify all unique polymorphisms in the drug-resistant mutants. In proof-of-principle studies with four different drug-resistant mutants, we explored the utility of this chemical-genomics approach. In particular, we discovered a new class of sterol-binding chemicals by linking the natural product theopalauamide to its cellular target in yeast, ergosterol.

## RESULTS

### Construction of a library of molecular barcoded yeast ORFs

The MoBY-ORF library consists of plasmids that each carry a pair of oligonucleotide barcodes and a single yeast ORF that is flanked by its native upstream and downstream genomic sequences. The plasmid vector p5472 carries a *URA3* selectable marker and a yeast centromere, which maintains one to three copies of the plasmid per cell (Fig. 1). The vector was designed to be compatible with an *in vivo* bacterial cloning method, mating-assisted genetically integrated cloning (MAGIC)<sup>18</sup>, which facilitates the rapid construction of recombinant DNA molecules, enabling the barcoded clones to be transferred efficiently to other vector backbones, such as a high-copy vector. The barcodes were obtained from the yeast deletion mutant collection<sup>19</sup> and comprise two unique 20-nucleotide DNA sequences (labeled the UPTAG and DNTAG) flanking a dominant selectable marker (*KanMX*) that confers resistance to the drug G418/kanamycin. The barcodes can be amplified with universal primers, enabling cells carrying a specific ORF to be quantitatively detected with a microarray having probes that hybridize to the barcode sequences<sup>20</sup>.

Each plasmid was constructed in a three-step process. First, each yeast ORF was PCR amplified from an average of ~900 bp upstream of the start codon to an average of ~250 bp downstream of the stop codon using a DNA template isolated from the sequenced S288C strain. The primers used are listed in Supplementary Tables 1 and 2 online. In addition, the *KanMX* barcode sequences that uniquely identify the ORF were PCR amplified from the appropriate strain in the yeast deletion collection. Second, the plasmid was assembled by homologous recombination by transforming yeast with the ORF, the barcode PCR products and linearized p5472 (Fig. 1 and Supplementary Fig. 1 online). Third, recombinant plasmids were recovered and used to transform bacteria to facilitate plasmid DNA isolation and subsequent diagnostic restriction digests to confirm the sizes of both fragments.

Each clone in the MoBY-ORF library was sequenced to confirm the 3' portion of the gene and the barcodes (summarized in Supplementary Table 3 online). We identified 4,396 ORFs (88.7%) with two unique barcodes, but 560 with only one barcode (344 with only an UPTAG and 216 with a DNTAG), as the other barcode was either not unique within the collection (that is, multiple clones contained the same barcode sequence), or it had no corresponding sequence on the Affymetrix TAG4 microarray<sup>20</sup>. In summary, the MoBY-ORF library version 1.0 contains 4,956 uniquely barcoded ORFs, representing ~90% of all non-dubious ORFs annotated in the *Saccharomyces* Genome Database (SGD). This collection will be available from Open Biosystems.

To assess the functionality of our clones, we first introduced 254 different MoBY-ORF plasmids into a synthetic genetic array (SGA)<sup>21</sup> query strain. We then used the SGA method to cross the plasmids into a set of corresponding temperature-sensitive mutants covering alleles of the same 254 essential genes, and tested the transformants for functional complementation at the restrictive temperatures. In total, 17 clones failed to rescue the temperature sensitivity of the corresponding mutant strain, suggesting that ~93% of the clones in the library should be functional (Supplementary Table 4 online).

### Combining MoBY-ORF complementation cloning and YTM

The method we used to clone drug-resistant genes by complementation with the MoBY-ORF library is shown in Figure 2. First, a recessive drug-resistant mutant associated with a single gene is isolated. Second, the drug-resistant mutant is transformed with the plasmid library—a starting culture of  $2 \times 10^6$  cells should include 400 clones of each of the ~5,000 different transformants in a pooled culture. Third, the transformants are pooled and grown in

either the presence or the absence of the drug. Fourth, the plasmids from the two pools are extracted and their barcodes are PCR amplified and then hybridized to a barcode microarray. This pooled growth strategy allows for simultaneous measurement of all transformants<sup>19,22</sup>. Because the wild-type copy of a drug-resistant gene will complement a recessive drug-resistant phenotype, its corresponding barcodes should be depleted relative to the others in the pool after growth in the presence of the drug.

To further pinpoint a high-confidence genetic locus associated with the drug-resistant mutation, we scanned for mutations across the genomes of both the parental strain and the drug-resistant mutant using a yeast tiling microarray (YTM) and the SNPScanner algorithm to identify single-nucleotide polymorphisms (SNPs)<sup>23</sup>. The YTM contained overlapping oligomers that cover the entire *S. cerevisiae* S288C reference genome enabling detection of ~85% of all SNPs<sup>23</sup>.

### Mapping cycloheximide- and rapamycin-resistant mutants

Cycloheximide is a well-characterized inhibitor of protein synthesis that binds to the ribosome. Mutations of glutamine-37 in Rpl28p, a component of the 60S ribosomal subunit, confer resistance to cycloheximide<sup>12,24</sup> and provided an excellent test case for our assay. As a proof of principle, we selected for spontaneous cycloheximide-resistant (*cyc*<sup>R</sup>) mutants and mapped the drug-resistant mutation through the combination of MoBY-ORF cloning by complementation and SNP scanning with the whole-genome YTM.

In the presence of cycloheximide, a MoBY-ORF transformed yeast strain that contained *RPL28* was depleted ~13-fold (that is, the strain grew poorly in the drug-treated culture relative to the untreated control) whereas the second-highest signal showed only ~1.3-fold depletion (Fig. 3a). YTM-based identification of SNPs in a *cyc*<sup>R</sup> mutant detected three signals that fulfilled the established prediction criteria for significant SNPs (Supplementary Table 5 online). One peak was located within the *RPL28* locus in the region encoding glutamine 37 (Fig. 3b). We sequenced the *RPL28* locus and identified a single-base substitution in residue 625, which generates a glutamine-37 substitution<sup>24</sup>. Thus, the YTM results support those of the MoBY-ORF library and together they provide independent evidence that a mutation in *RPL28* confers cycloheximide resistance.

To further characterize our mapping system, we isolated a mutant resistant to rapamycin, a natural product isolated from *Streptomyces hygroscopicus* with antifungal and immunosuppressant activities<sup>25</sup>. Rapamycin binds to the FKBP12 peptidyl-prolyl *cis-trans* isomerase (PPIase) to form a complex that inhibits TOR kinases, which regulate a wide range of functions including cell growth, proliferation and protein synthesis<sup>15,26–28</sup>. Mutations in FKBP12 (encoded by *FPR1* in yeast) and in the TOR kinases (encoded by *TOR1* and *TOR2* in yeast) confer resistance to rapamycin<sup>15</sup>. Genetic analysis showed that our rapamycin-resistant (*rap*<sup>R</sup>) mutant was recessive and associated with a single gene (data not shown).

Using MoBY-ORF complementation cloning, we found that cells transformed with a plasmid carrying *FPR1* were depleted by ~28-fold in the presence of rapamycin, whereas the strain with the second-highest signal showed only ~1.7-fold depletion (Fig. 3c). To confirm that the wild-type copy of *FPR1* restored the rapamycin sensitivity of the drug-resistant mutant we directly transformed the *rap*<sup>R</sup> mutant with an individual *FPR1* plasmid (data not shown). We also detected six significant SNPs in the *rap*<sup>R</sup> mutant using the YTM (Supplementary Table 5), including a single peak at the *FPR1* locus (Fig. 3d). Sequencing of the *FPR1* locus from the *rap*<sup>R</sup> mutant identified a 29 base-pair deletion spanning nucleotides 282 and 310 of *FPR1*, which coincided with the peak signal from the YTM. Thus, the

combined results of the MoBY-ORF complementation cloning and the YTM analysis identified *FPR1* as the mutant gene conferring rapamycin-resistance.

### Mapping a sordarin-resistant mutant

Sordarin is a natural product produced by a species of fungus in the genus *Sordaria*<sup>29,30</sup>. In budding yeast, it specifically inhibits fungal translation by binding to and stabilizing the eEF2-GDP-ribosome complex<sup>11,31</sup>. Mutations in *EFT2*, which encodes elongation factor 2, have been shown to confer resistance to sordarin<sup>11</sup>. We did not isolate spontaneous sordarin-resistant mutants using our standard protocol. Therefore, to enrich for mutants, we attempted to isolate sordarin-resistant mutants in a yeast strain carrying an *msh2Δ* mutation, which deletes a gene involved in mismatch repair and leads to a higher rate of mutation<sup>32</sup>. Using the *msh2Δ* strain, we routinely isolated drug-resistant mutants using approximately tenfold fewer cells compared to the wild-type strain. We examined one sordarin-resistant mutant in detail and confirmed that the drug-resistant phenotype was recessive and associated with a single gene (data not shown).

Using MoBY-ORF, the strongest signal was obtained from a yeast strain transformed with a plasmid carrying *EFT2*, which was depleted approximately twofold in the competitive growth assay (Fig. 3e). This modest depletion, near the limit of detection in this assay, may reflect the fact that the *EFT2* gene is associated with only one unique barcode, which moreover contains a single-nucleotide mismatch to the probe on the array. To be confident of this result, we confirmed the complementation result by individual transformation (Supplementary Fig. 2 online). The YTM analysis of *sor<sup>R</sup>* mutant identified five significant SNPs throughout the genome, but did not detect a polymorphism in *EFT2* (Supplementary Table 5). This is probably because the majority of the probes covering *EFT2* are not unique on the YTM. The sequence of the paralog *EFT1* is virtually identical to *EFT2*, which means there would be substantial cross-hybridization, confounding detection. Direct sequence analysis of the *EFT2* locus from the *sor<sup>R</sup>* mutant identified a single base-pair substitution mutation at nucleotide 1568 of *EFT2*. This mutation leads to an altered protein where serine 523 of Eft2p is substituted with tyrosine (Eft2p-S523Y), a result that is consistent with previous observations that substitutions in this region of Eft2p, encompassing residues 517 to 524, confer sordarin resistance<sup>11</sup>. Thus, the MoBY-ORF approach enables us to identify and, at least in some cases, distinguish drug-resistant mutations in paralogs.

### Theopalauamide and stichloroside have a common target

Theopalauamide and stichloroside are two natural products with potent antifungal activities but uncharacterized MOAs<sup>9</sup>. Theopalauamide was isolated from a bacterial symbiont of a marine sponge from Indonesia, whereas stichloroside was isolated from a marine sea cucumber from The Commonwealth of Dominica<sup>9</sup>. Previously, we showed that these two compounds display highly similar chemical-genetic profiles when testing the set of ~5,000 viable deletion mutants for hypersensitivity (Fig. 4a), which suggested that they have the same MOA<sup>9</sup>. This is a surprising result because theopalauamide and stichloroside have highly dissimilar chemical structures<sup>9</sup>. Nevertheless, consistent with a common MOA, we isolated a mutant resistant to stichloroside and found that the same mutant was also resistant to theopalauamide<sup>9</sup>.

Because we had only a limited amount of these two natural products, the MoBY-ORF library was critical for cloning the gene associated with the drug-resistant phenotype of the theopalauamide/stichloroside-resistant (*theo<sup>R</sup>*) mutant. Using the MoBY-ORF complementation assay, we identified a plasmid carrying *MVD1* (Fig. 4b and Supplementary Fig. 3 online), which encodes mevalonate pyrophosphate decarboxylase—an essential enzyme involved in an early step of the ergosterol biosynthesis pathway. YTM analysis

failed to detect a polymorphism in *MVD1*, probably because this particular region of the YTM is unusual and lacks the probe density required for the SNPScanner algorithm. In this case, we did not detect any other polymorphisms in the *theo*<sup>R</sup> mutant compared to the parental strain (Supplementary Fig. 4 online and Supplementary Table 5). Sequencing of the *theo*<sup>R</sup>*MVD1* locus identified a single nucleotide substitution within the active site of the enzyme that results in lysine to asparagine mutation at residue 18 (Mvd1p-K18N).

We tested two hypotheses for the MOAs of theopalauamide and stichloroside that could explain why the *theo*<sup>R</sup> Mvd1p-K18N substitution leads to a drug-resistant phenotype. First, these drugs may directly inhibit the enzymatic activity of Mvd1p by binding to its active site in a K18N-dependent manner<sup>33</sup>. Alternatively, these drugs may target the products of the Mvd1p pathway—mainly ergosterol—and the active site mutation may decrease Mvd1p activity, resulting in lower levels of ergosterol that render the cells drug resistant. This second hypothesis is consistent with the MOA of other natural products that bind specific lipids and kill cells by disrupting the integrity of the plasma membrane<sup>9</sup>.

To distinguish between these two hypotheses, we examined a temperature-sensitive yeast strain, *mvd1-ts*, that contains a hypomorphic allele of *MVD1* that is mutated outside the active site pocket (Mvd1p-I35K)<sup>33</sup>. If theopalauamide and stichloroside target Mvd1p directly, a strain carrying an *MVD1* hypomorph should be more sensitive to the drugs. Conversely, if the drugs target a product of the *MVD1* pathway, a hypomorphic mutant should show more drug resistance than wild type. Consistent with the product-targeting hypothesis, *mvd1-ts* grown at a semi-permissive temperature was resistant to both theopalauamide and stichloroside (Fig. 4c). Similarly, a strain carrying a different *MVD1* hypomorphic allele—an *mvd1-DAmP* mutant expressing less wild-type protein owing to a deletion of the 3' untranslated region of *MVD1* that reduces mRNA tenfold<sup>34,35</sup>—was also resistant to theopalauamide (data not shown). In contrast, the DAmP alleles of genes directly targeted by drugs are often hypersensitive to the drug<sup>36</sup>, presumably because there is less of the drug target in the cell. Taken together, our results indicate that reduced Mvd1p activity, which should lower cellular ergosterol levels, appears to lead to the drug-resistant phenotype.

To lend further support to the hypothesis that theopalauamide targets a product of the *MVD1* pathway, we tested whether the *theo*<sup>R</sup> mutant was resistant to other compounds that bind sterols, such as amphotericin B and nystatin. Indeed, we found that *theo*<sup>R</sup> was partially resistant to amphotericin B, although we failed to detect nystatin resistance (Supplementary Fig. 5 online). Moreover, as Mvd1p is required early in the ergosterol biosynthetic pathway, the product-targeting hypothesis would predict that defects in later biosynthetic stages should also confer theopalauamide resistance. Indeed, we confirmed that deletion mutants, *erg2Δ* and *erg3Δ*, which participate in third and the fourth last steps of ergosterol biosynthesis, were resistant to theopalauamide (data not shown).

To indirectly test whether theopalauamide and stichloroside bind to ergosterol, we added exogenous ergosterol to cultures containing toxic levels of these compounds (Fig. 4d). We also examined, as controls for this experiment, the effect of exogenous ergosterol on the toxicity of amphotericin B, a sterol-binding antifungal compound, and ketoconazole, an antifungal compound that inhibits Erg1p, another ergosterol biosynthetic enzyme (Fig. 4d). Exogenous ergosterol rescued the toxicity of theopalauamide, stichloroside and amphotericin B, but had no effect on ketoconazole's toxicity, suggesting that, like amphotericin B, both theopalauamide and stichloroside may interact physically with ergosterol. Interestingly, cholesterol behaved similarly in this assay, indicating that the general sterol backbone is responsible for the activity (data not shown).

To further show that theopalauamide and stichloroside interact with ergosterol, we studied the effect of these compounds on fluorescent marker release from phosphatidylcholine liposomes that contained various levels of ergosterol. Theopalauamide (10  $\mu\text{g/ml}$ ) caused a maximal  $\sim 30\%$  leakage of liposomes containing 20% ergosterol, whereas it had no effect on liposomes lacking ergosterol (Fig. 4e,f and Supplementary Fig. 6a,b online). Although we could not detect more than  $\sim 30\%$  leakage, this effect was highly specific to ergosterol. Stichloroside caused ergosterol-enhanced leakage (Supplementary Fig. 7a,b online), but it was more potent, as was nystatin, another sterol-binding antifungal compound (data not shown). Thus, both theopalauamide and stichloroside disrupt ergosterol-containing membranes specifically.

### Theopalauamide belongs to a novel class of sterol-binding compound

Sterol-binding compounds fall into two well-characterized classes. The polyene class is the most common (Fig. 5a) and includes amphotericin B and nystatin<sup>37</sup>. Another is the saponin class (Fig. 5a), which includes steroidal glycosides and steroidal glycoalkaloids, such as  $\alpha$ -tomatine<sup>38,39</sup>. Saponins are often derived from plants and they interact with sterol-containing membranes causing membrane permeabilization, which is thought to be partly responsible for defending against fungal pathogens<sup>39,40</sup>. Closer examination of the stichloroside structure revealed that it is, in fact, a member of the saponin class, containing a lanostane-type triterpene framework<sup>41</sup>. Interestingly, theopalauamide does not resemble any known sterol-binding chemical and therefore may represent a novel class of sterol-binding compound.

Theopalauamide is structurally related to theonellamides (Fig. 5a)<sup>42,43</sup> and theonegramide<sup>44</sup>, compounds isolated from other marine sponges of the genus *Theonella*. This family of antifungal metabolites shares an unusual bicyclic structure bridged by a histidinoalanine residue. Evidence to support the possibility that these metabolites represent a new class of sterol-binding compound was obtained from an independent study in which it was discovered that theonellamide targets sterols in the fission yeast, *Schizosaccharomyces pombe* (S.N. and M.Y., unpublished data).

To investigate whether theonellamide also binds to ergosterol in *S. cerevisiae*, we found that fluorescently labeled theonellamide A (Supplementary Fig. 8 online) bound to ergosterol specifically in an *in vitro* lipid-binding assay (Fig. 5b). In addition, we found that, our previously isolated theopalauamide-resistant strain (*theo*<sup>R</sup>) was resistant to theonellamide A, which is toxic to wild-type *S. cerevisiae* (Fig. 5c). Finally, to test whether theonellamide binds to ergosterol in the yeast plasma membrane, we found that fluorescently labeled theonellamide A stained the cell surface of wild-type budding yeast (as expected)<sup>45</sup>, with a polarized staining pattern to the shmoo tip consistent with the localization pattern of filipin, a fluorescent sterol-binding compound<sup>46</sup>, but only weakly stained the plasma membrane of *theo*<sup>R</sup> mutant cells (Fig. 5d). Quantification revealed that staining was reduced to  $\sim 15\%$  wild-type levels (data not shown). Taken together, our results suggest that theopalauamide and theonellamide define a novel class of sterol-binding compound. However, further analysis is required to fully characterize the specificity of their lipid-binding properties and the mechanism of their antifungal activity.

## DISCUSSION

We developed an efficient chemical-genomic approach for linking bioactive compounds to aspects of MOAs, including targets. An essential element of this approach was the construction of the MoBY-ORF library, designed in part to facilitate the cloning of wild-type versions of drug-resistant mutant genes by complementation with a minimal amount of bioactive compound. This library contains four important features. First, expression of every

ORF is driven by its endogenous promoter and its normal 3'UTR, which should preserve its normal expression pattern. Second, most of the plasmids are barcoded by two unique 20-bp oligonucleotides, which enables measurement of the relative abundance of a specific transformant using a barcode microarray and facilitates parallel analysis of all transformants in a pool simultaneously. Third, the majority of the MoBY-ORF clones contain only a single ORF, which streamlines analysis compared with genomic DNA libraries derived from random fragments<sup>2,47</sup>. Fourth, the gene fragment and the barcodes of each clone can be transferred efficiently to another plasmid backbone, such as a high-copy vector, using the MAGIC system<sup>18</sup>.

This study validates the use of the MoBY-ORF library for cloning by complementation with a barcode microarray readout. But there are several potential variations of this method. For example, measuring barcode abundance by deep sequencing may increase the resolution of the barcode assay<sup>48,49</sup>. The ORF fragment itself could be PCR amplified and used as an identifier in combination with an ORF-based microarray format. Complementation cloning has been carried out with a galactose-inducible yeast ORF library, using the ORF fragment as an identifier<sup>4</sup>, but this system is not ideal because the genes are highly expressed in a deregulated manner, which is often associated with a dosage lethality phenotype<sup>50,51</sup>.

Cloning by complementation requires that the drug-resistant mutant be at least partially recessive. In theory, we may not be able to identify a drug-resistant mutant that carries a fully dominant mutation, such as one that occurs in the primary drug target and prevents drug binding. However, two observations suggest that the potential dominance problem is not a major concern. First, in most cases, recessive mutations can be identified in drug-target genes<sup>9-15</sup>. Also, many proteins function in complexes and thus when cells carry both a mutated and a wild-type copy of the gene, both drug-sensitive and drug-resistant complexes would exist, leading to increased drug sensitivity. For example, most of the mutations conferring resistance to drugs that target the ribosome and prevent drug-binding are recessive. Second, most dominant mutations actually display some recessive character. Because the cloning by complementation in a pooled format involves competitive growth, strains with as little as a 5% slower growth-rate difference should be cleared from the population within twenty generations<sup>52</sup>. Thus, as long as the 'recessiveness' of the mutation means that the cells carrying a wild-type copy of the gene show reduced fitness compared to those with other unrelated genes, the barcode microarray assay should be sensitive enough to identify the complementing gene. Finally, for dominant mutations that cannot be identified with our MoBY-ORF approach, YTM analysis, deep sequencing<sup>48,49</sup> or high-resolution genetic mapping<sup>53</sup> offer other potential ways to identify a dominant drug-resistant mutation.

Cloning by complementation with the MoBY-ORF library is a portable assay that can be carried out with any *S. cerevisiae* strain. Different genetic backgrounds that increase either the spontaneous mutation rate or drug sensitivity<sup>54</sup> should enhance the efficiency of the procedure because they reduce the amount of compound required for the assay. There is also the potential for identifying compound-specific hypersensitive strain backgrounds for drug-resistant mutant analysis by first conducting chemical-genetic profiling with the set of ~5,000 viable deletion mutant strains.

We expect that the MoBY-ORF collection will facilitate other assays beyond MOA studies. In principle, our complementation method is amenable to any recessive phenotype. This collection should also enable studies of gene dosage phenotypes in which the number of copies of each gene can be controlled with much greater precision. For example, dosage resistance analysis could be carried out with the MoBY-ORF library, monitoring the drug resistance phenotype associated with one extra copy of each gene. Moreover, a growing



body of literature has pointed to the selective advantage of amplified genomic fragments under different conditions<sup>55-57</sup>, and the targets of selection within these amplified fragments might be identified by following the fitness profiles of a pooled population of transformants under the same conditions.

Yeast chemical-genomic approaches have been shown to be effective for deciphering MOAs and targets and may be especially effective for studying natural products, which are often complicated molecules with highly selected targets. Here, we discovered that theopalauamide and theonellamide represent a new class of sterol-binding compound, providing a chemical means for exploring the cellular localization and function of sterols. Large-scale application of yeast chemical-genomics approaches should expand our catalog of specific chemical probes for research and drug discovery.

## METHODS

The MoBY-ORF collection will be available through Open Biosystems. The Supplementary Methods online lists the strains used in this study, growth media, plasmid pool preparation method, MoBY-ORF clone construction methods and analysis, procedures for sequencing of the MoBY-ORF collection, procedures for functional complementation analysis of essential genes with MoBY-ORF plasmids and preparation of Theonellamide-AMCA.

### Chemicals

Cycloheximide (C1988), sordarin (S1422) and ergosterol (E6510) were purchased from Sigma. Rapamycin (R1018) was purchased from AG Scientific. Theopalauamide and stichloroside were purified from natural extracts using methanol extraction<sup>58</sup>. Theonellamide was a kind gift from S. Matsunaga. Cycloheximide was dissolved in water as a 10 mg/ml stock. Rapamycin, sordarin, theopalauamide and stichloroside were dissolved in DMSO as a 10 mg/ml stocks. Theonellamide was dissolved in 70% aqueous DMSO as 1 mg/ml stock.

### Cloning by complementation with the MoBY-ORF library

Each drug-resistant mutant was transformed with MoBY-ORF v1; ~50,000 individual transformants were obtained and pooled together. Each transformant pool was frozen in 20% glycerol. A sample of the frozen transformant pool was subsequently grown in 50 ml of YEPD with G418 (100  $\mu$ g/ml), either in the presence or absence of compound, with a starting OD<sub>600</sub> = 0.0625. A standard growth assay was performed on wild-type and drug-resistant mutants at different drug concentrations. The concentration of the compound that produced the largest difference in the growth rate between the wild-type and drug-resistant mutant was chosen for the complementation assay. Each pool was grown for 7 generations and then diluted in fresh medium to OD<sub>600</sub> = 0.0625 (50 ml). After 13 more generations, the cells derived from the saturated cultures were harvested and stored frozen in ~20% glycerol at -80 °C.

### Plasmid isolation from yeast

The plasmids from the transformant pool were extracted by a modified miniprep protocol using the Qiagen miniprep kit as described<sup>59</sup>.

### Yeast barcode microarray hybridization and data analysis

PCR amplification of the barcodes and microarray hybridization were performed as described<sup>60</sup>. Each drug-treated array was quartile normalized against the solvent-treated array. The fold-change ( $\log_2$  solvent/drug) was calculated using the normalized data. The UPTAGs and DOWNTAGs were normalized separately and the tag with the highest  $\log_2$

ratio was chosen to represent that particular clone. Two biological replicates were performed for each experiment. The mean  $\log_2$  ratio of each clone was calculated from the maximum value from each replicate. A reference key file for the Affymetrix TAG4 microarray MoBY-ORF barcode annotation can be found in Supplementary Table 6 online.

### Yeast whole-genome tiling microarray

We prepared genomic DNA from a single clonal isolate using the Qiagen Genomic-Tip 500/G according to the manufacturer's guidelines. Genomic DNA was randomly fragmented using sonication and labeled subsequently with a biotinylated nucleotide using random primed Klenow labeling, at 25 °C for 16 h with a Bioprime Labeling Kit (Invitrogen). Labeled DNA was hybridized to the *S. cerevisiae* Tiling 1.0R Array (Affymetrix) as described<sup>23</sup>. The data were analyzed using the SNPScanner algorithm<sup>23</sup>.

### Isolation of drug-resistant mutants

A culture containing a total of  $2 \times 10^7$  wild-type cells was spread on a YEPD + drug agar plate (10  $\mu\text{g}/\text{ml}$  for cycloheximide, 50  $\mu\text{g}/\text{ml}$  for rapamycin and 50  $\mu\text{g}/\text{ml}$  for sordarin). Resistant colonies were usually apparent after 2 or 3 d at 30 °C. In each case, a single mutant was subject to standard yeast genetic analysis, which confirmed that the mutations were recessive and associated with a single gene.

### Yeast fitness assays

All yeast growth assays were performed in 96-well microtiter plates in YEPD, either with or without drug. The starting  $\text{OD}_{600}$  was 0.0625 and the volume was 100  $\mu\text{l}$ . The yeast strains were grown, shaking, for 16 h at 30 °C and the  $\text{OD}_{600}$  was recorded after 16 h.

### Liposome leakage assay

Large unilamellar vesicles (LUVs, 100 nm diameter) were prepared by filter extrusion through 100 nm polycarbonate filters in the presence of 5 mM calcein, a fluorescent compound that self-quenches at high concentrations. LUVs were prepared from phosphatidylcholine (PC, from egg yolk, Type XVI-E, Sigma-Aldrich) with 0 to 40% ergosterol (Sigma-Aldrich) and dialyzed overnight to remove external, untrapped calcein. Leakage of calcein from the liposomes was measured by increase in fluorescence (reduction of quenching upon dilution) at 23 °C in 2 ml of TNE (10 mM Tris-Cl pH 7.4, 154 mM NaCl, and 0.1 mM EDTA) containing ~50  $\mu\text{g}$  LUVs. Base-line fluorescence of LUVs was determined before stichloroside or theopalauamide addition and 100% leakage determined by addition of Triton X-100 to 0.1% after 3 min of incubation with stichloroside or theopalauamide.

### *In vitro* ergosterol binding assay

Binding of theonellamide (TNM), as a TNM-AMCA derivative, to various lipids was evaluated in a 96-well microtiter plate. The wells of the microtiter plates (Immulon 1B, Thermo Fisher Scientific) were coated with 50  $\mu\text{l}$  of lipid solution (10  $\mu\text{M}$  of PC, PE (1,2-dimyristoyl-*sn*-glycero-3-phosphoethanolamine), PS (1,2-dimyristoyl-*sn*-glycero-3-phospho-*L*-serine), sterols, or 10  $\mu\text{g}/\text{ml}$  of SM (chicken egg yolk sphingomyelin) in ethanol by evaporating at 30 °C for 2 h. After blocking the wells with Tris-buffered saline (TBS, 10 mM Tris-HCl, pH 7.4, 150 mM NaCl), containing 1% of BSA for 1 h at 30 °C, the wells were incubated with TNM-AMCA (0.5  $\mu\text{M}$ ) in TBS containing 1% BSA for 2 h at 30 °C. After washing the wells two times with TBS containing 1% BSA, the bound TNM-AMCA was dissolved with 50  $\mu\text{l}$  of DMSO, 40  $\mu\text{l}$  of which was transferred to another 96-well plate (FIA black module plate, Greiner Bio-One) to measure the bound fluorescence (ex., 345 nm; em., 450 nm) using a microplate reader SpectraMax M2e (Molecular Devices). PC (1,2-

dimyristoyl-*sn*-glycero-3-phosphocholine) and PE were purchased from Wako Pure Chemical Industries. PS and SM were from Sigma. Ergosterol was from Nacalai Tesque.

### ***In vivo* staining of yeast cells with theonellamide-AMCA**

Overnight cultures of wild-type yeast cells were diluted to OD<sub>600</sub> = 0.1 and grown at 30 °C for 2 h. For  $\alpha$ -factor treatment,  $\alpha$ -factor was added to the culture medium to a final concentration of 5  $\mu$ M and the cells were grown for another 2 h. Cells were stained with Theonellamide-AMCA (10  $\mu$ g/ml) for 15 min (for  $\alpha$ -factor treatment) or 1 h (with no  $\alpha$ -factor treatment). Cells were then washed with low-fluorescence medium and images were taken with a Quorum Wave FX spinning Disc Confocal System microscope using a 63 $\times$  objective. Fluorescently-bound theonellamide-AMCA was detected using the DAPI channel (ex., 345 nm; em., 450 nm).

### **Supplementary Material**

Refer to Web version on PubMed Central for supplementary material.

### **Acknowledgments**

We thank A. Smith and L. Heisler for advice on the data analysis of barcode microarray and A. Ward for technical assistance with the YTM experiments. We thank B. Sheikh for primer design, diagnostic digest predictions and sequencing scripts. We thank K. Toufighi for data analysis of liposome leakage experiments. Theonellamide was a kind gift from S. Matsunaga (Graduate School of Agricultural and Life Sciences, The University of Tokyo). L.M. was supported by a Canadian Institutes of Health Research Doctoral Research Award. R.J.A. was supported by a research grant from NSERC. C.N. was supported by NHGRI (MOP-84305). G.G. was supported by NHGRI (MOP-81340). D.B. was supported by NIGMS Center for Quantitative Biology (GM071508) and R01 (GM046406). T.R.G. was supported by National Institutes of Health (GM62637). M.Y. and S.N. were supported by an Energy and Industrial Technology Development Organization (NEDO) project on development of basic technology to control biological systems using chemical compounds. C.B. was supported by Genome Canada through the Ontario Genomics Institute as per research agreement 2004-OGI-3-01 and Canadian Institutes of Health Research agreement number MOP-57830.

### **References**

1. Giaever G, et al. Genomic profiling of drug sensitivities via induced haploinsufficiency. *Nat. Genet.* 1999; 21:278–283. [PubMed: 10080179]
2. Hoon S, et al. An integrated platform of genomic assays reveals small-molecule bioactivities. *Nat. Chem. Biol.* 2008; 4:498–506. [PubMed: 18622389]
3. Rine J, Hansen W, Hardeman E, Davis RW. Targeted selection of recombinant clones through gene dosage effects. *Proc. Natl. Acad. Sci. USA.* 1983; 80:6750–6754. [PubMed: 6316322]
4. Butcher RA, et al. Microarray-based method for monitoring yeast overexpression strains reveals small-molecule targets in TOR pathway. *Nat. Chem. Biol.* 2006; 2:103–109. [PubMed: 16415861]
5. Luesch H, et al. A genome-wide overexpression screen in yeast for small-molecule target identification. *Chem. Biol.* 2005; 12:55–63. [PubMed: 15664515]
6. Parsons AB, et al. Integration of chemical-genetic and genetic interaction data links bioactive compounds to cellular target pathways. *Nat. Biotechnol.* 2004; 22:62–69. [PubMed: 14661025]
7. Hillenmeyer ME, et al. The chemical genomic portrait of yeast: uncovering a phenotype for all genes. *Science.* 2008; 320:362–365. [PubMed: 18420932]
8. Hughes TR, et al. Functional discovery via a compendium of expression profiles. *Cell.* 2000; 102:109–126. [PubMed: 10929718]
9. Parsons AB, et al. Exploring the mode-of-action of bioactive compounds by chemical-genetic profiling in yeast. *Cell.* 2006; 126:611–625. [PubMed: 16901791]
10. Douglas CM, et al. The *Saccharomyces cerevisiae* FKS1 (ETG1) gene encodes an integral membrane protein which is a subunit of 1,3-beta-D-glucan synthase. *Proc. Natl. Acad. Sci. USA.* 1994; 91:12907–12911. [PubMed: 7528927]

11. Justice MC, et al. Elongation factor 2 as a novel target for selective inhibition of fungal protein synthesis. *J. Biol. Chem.* 1998; 273:3148–3151. [PubMed: 9452424]
12. Fried HM, Warner JR. Molecular cloning and analysis of yeast gene for cycloheximide resistance and ribosomal protein L29. *Nucleic Acids Res.* 1982; 10:3133–3148. [PubMed: 6285288]
13. Liu Y-X, Hsiung Y, Jannatipour M, Yeh Y, Nitiss JL. Yeast topoisomerase II mutants resistant to anti-topoisomerase agents: identification and characterization of new yeast topoisomerase II mutants selected for resistance to etoposide. *Cancer Res.* 1994; 54:2943–2951. [PubMed: 8187080]
14. Kanik-Ennulat C, Montalvo E, Neff N. Sodium orthovanadate-resistant mutants of *Saccharomyces cerevisiae* show defects in golgi-mediated protein glycosylation, sporulation and detergent resistance. *Genetics.* 1995; 140:933–943. [PubMed: 7672592]
15. Heitman J, Movva N, Hall M. Targets for cell cycle arrest by the immunosuppressant rapamycin in yeast. *Science.* 1991; 253:905–909. [PubMed: 1715094]
16. Wiesen KM, Xia S, Yang C-PH, Horwitz SB. Wild-type class I [beta]-tubulin sensitizes Taxol-resistant breast adenocarcinoma cells harboring a [beta]-tubulin mutation. *Cancer Lett.* 2007; 257:227–235. [PubMed: 17869412]
17. Douglas CM, Marrinan JA, Li W, Kurtz MB. A *Saccharomyces cerevisiae* mutant with echinocandin-resistant 1,3-beta-D-glucan synthase. *J. Bacteriol.* 1994; 176:5686–5696. [PubMed: 8083161]
18. Li MZ, Elledge SJ. MAGIC, an *in vivo* genetic method for the rapid construction of recombinant DNA molecules. *Nat. Genet.* 2005; 37:311–319. [PubMed: 15731760]
19. Giaever G, et al. Functional profiling of the *Saccharomyces cerevisiae* genome. *Nature.* 2002; 418:387–391. [PubMed: 12140549]
20. Pierce SE, et al. A unique and universal molecular barcode array. *Nat. Methods.* 2006; 3:601–603. [PubMed: 16862133]
21. Tong AHY, et al. Systematic genetic analysis with ordered arrays of yeast deletion mutants. *Science.* 2001; 294:2364–2368. [PubMed: 11743205]
22. Winzler EA, et al. Functional characterization of the *S. cerevisiae* genome by gene deletion and parallel analysis. *Science.* 1999; 285:901–906. [PubMed: 10436161]
23. Gresham D, et al. Genome-wide detection of polymorphisms at nucleotide resolution with a single DNA microarray. *Science.* 2006; 311:1932–1936. [PubMed: 16527929]
24. Käufer NF, Fried HM, Schwindinger WF, Jasin M, Warner JR. Cycloheximide resistance in yeast: the gene and its protein. *Nucleic Acids Res.* 1983; 11:3123–3135. [PubMed: 6304624]
25. Vézina C, Kudelski A, Sehgal SN. Rapamycin (AY-22,989), a new antifungal antibiotic. I. Taxonomy of the producing streptomycete and isolation of the active principle. *J. Antibiot. (Tokyo).* 1975; 28:721–726. [PubMed: 1102508]
26. Brown EJ, et al. A mammalian protein targeted by G1-arresting rapamycin-receptor complex. *Nature.* 1994; 369:756–758. [PubMed: 8008069]
27. Chiu MI, Katz H, Berlin V. RAPT1, a mammalian homolog of yeast Tor, interacts with the FKBP12/rapamycin complex. *Proc. Natl. Acad. Sci. USA.* 1994; 91:12574–12578. [PubMed: 7809080]
28. Sabatini DM, Erdjument-Bromage H, Lui M, Tempst P, Snyder SH. RAFT1: A mammalian protein that binds to FKBP12 in a rapamycin-dependent fashion and is homologous to yeast TORs. *Cell.* 1994; 78:35–43. [PubMed: 7518356]
29. Coval SJ, Puar MS, Phife DW, Terracciano JS, Patel M. SCH57404, an antifungal agent possessing the rare sodaricin skeleton and a tricyclic sugar moiety. *J. Antibiot. (Tokyo).* 1995; 48:1171–1172. [PubMed: 7490228]
30. Hauser D, Sigg HP. Isolierung und abbau von sordarin. 1. Mitteilung über sordarin. *Helv. Chim. Acta.* 1971; 54:1178–1190. [PubMed: 5095217]
31. Capa L, Mendoza A, Lavandera JL, Gomez de las Heras F, Garcia-Bustos JF. Translation elongation factor 2 is part of the target for a new family of antifungals. *Antimicrob. Agents Chemother.* 1998; 42:2694–2699. [PubMed: 9756779]
32. Drotschmann K, et al. Mutator phenotypes of yeast strains heterozygous for mutations in the MSH2 gene. *Proc. Natl. Acad. Sci. USA.* 1999; 96:2970–2975. [PubMed: 10077621]

33. Krepiy D, Miziorko HM. Identification of active site residues in mevalonate diphosphate decarboxylase: implications for a family of phosphotransferases. *Protein Sci.* 2004; 13:1875–1881. [PubMed: 15169949]
34. Schuldiner M, et al. Exploration of the function and organization of the yeast early secretory pathway through an epistatic miniarray profile. *Cell.* 2005; 123:507–519. [PubMed: 16269340]
35. Muhlrad D, Parker R. Aberrant mRNAs with extended 3' UTRs are substrates for rapid degradation by mRNA surveillance. *RNA.* 1999; 5:1299–1307. [PubMed: 10573121]
36. Yan Z, et al. Yeast Barcoders: a chemogenomic application of a universal donor-strain collection carrying bar-code identifiers. *Nat. Methods.* 2008; 5:719–725. [PubMed: 18622398]
37. Bolard J. How do the polyene macrolide antibiotics affect the cellular membrane properties? *Biochim. Biophys. Acta.* 1986; 864:257–304. [PubMed: 3539192]
38. Arneson PA, Durbin RD. Studies on the mode of action of tomatine as a fungitoxic agent. *Plant Physiol.* 1968; 43:683–686. [PubMed: 5661492]
39. Simons V, et al. Dual effects of plant steroidal alkaloids on *Saccharomyces cerevisiae*. *Antimicrob. Agents Chemother.* 2006; 50:2732–2740. [PubMed: 16870766]
40. Keukens EAJ, et al. Dual specificity of sterol-mediated glycoalkaloid induced membrane disruption. *Biochim. Biophys. Acta.* 1992; 1110:127–136. [PubMed: 1390841]
41. Kitagawa I, Kobayashi M, Inamoto T, Yasuzawa T, Kyogoku Y. The structures of 6 antifungal oligoglycosides, stichloroside-a1, stichloroside-a2, stichloroside-b1, stichloroside-b2, stichloroside-c1, and stichloroside-c2, from the sea-cucumber *stichopus-chloronotus* (brandt). *Chem. Pharm. Bull. (Tokyo).* 1981; 29:2387–2391.
42. Matsunaga S, Fusetani N, Hashimoto K, Walchli M, Theonellamide F. A novel antifungal bicyclic peptide from a marine sponge *Theonella* sp. *J. Am. Chem. Soc.* 1989; 111:2582–2588.
43. Matsunaga S, Fusetani N. Theonellamides A-E, cytotoxic bicyclic peptides, from a marine sponge *Theonella* sp. *J. Org. Chem.* 1995; 60:1177–1181.
44. Bewley CA, Faulkner DJ. Theonegramide, an antifungal glycopeptide from the Philippine lithistid sponge *theonella swinhoei*. *J. Org. Chem.* 1994; 59:4849–4852.
45. Ott RG, et al. Flux of sterol intermediates in a yeast strain deleted of the lanosterol C-14 demethylase Erg11p. *Biochim. Biophys. Acta.* 2005; 1735:111–118. [PubMed: 15951236]
46. Bagnat M, Simons K. Cell surface polarization during yeast mating. *Proc. Natl. Acad. Sci. USA.* 2002; 99:14183–14188. [PubMed: 12374868]
47. Jones GM, et al. A systematic library for comprehensive overexpression screens in *Saccharomyces cerevisiae*. *Nat. Methods.* 2008; 5:239–241. [PubMed: 18246075]
48. Shendure J, Ji H. Next-generation DNA sequencing. *Nat. Biotechnol.* 2008; 26:1135–1145. [PubMed: 18846087]
49. Kahvejian A, Quackenbush J, Thompson JF. What would you do if you could sequence everything? *Nat. Biotechnol.* 2008; 26:1125–1133. [PubMed: 18846086]
50. Deutschbauer AM, et al. Mechanisms of haploinsufficiency revealed by genome-wide profiling in yeast. *Genetics.* 2005; 169:1915–1925. [PubMed: 15716499]
51. Sopko R, et al. Mapping pathways and phenotypes by systematic gene overexpression. *Mol. Cell.* 2006; 21:319–330. [PubMed: 16455487]
52. Smith V, Botstein D, Brown PO. Genetic footprinting: a genomic strategy for determining a gene's function given its sequence. *Proc. Natl. Acad. Sci. USA.* 1995; 92:6479–6483. [PubMed: 7604017]
53. Jorgensen P, et al. High-resolution genetic mapping with ordered arrays of *Saccharomyces cerevisiae* deletion mutants. *Genetics.* 2002; 162:1091–1099. [PubMed: 12454058]
54. Rogers B, et al. The pleiotropic drug ABC transporters from *Saccharomyces cerevisiae*. *J. Mol. Microbiol. Biotechnol.* 2001; 3:207–214. [PubMed: 11321575]
55. Rancati G, et al. Aneuploidy underlies rapid adaptive evolution of yeast cells deprived of a conserved cytokinesis motor. *Cell.* 2008; 135:879–893. [PubMed: 19041751]
56. Dunham MJ, et al. Characteristic genome rearrangements in experimental evolution of *Saccharomyces cerevisiae*. *Proc. Natl. Acad. Sci. USA.* 2002; 99:16144–16149. [PubMed: 12446845]

57. Gresham D, et al. The repertoire and dynamics of evolutionary adaptations to controlled nutrient-limited environments in yeast. *PLoS Genet.* 2008; 4:e1000303. [PubMed: 19079573]
58. Williams DE, et al. Dominicin, a cyclic octapeptide, and laughine, a bromopyrrole alkaloid, isolated from the Caribbean marine sponge *Eurypon laughlini*. *J. Nat. Prod.* 2005; 68:327–330. [PubMed: 15787430]
59. Butcher RA, Schreiber SL. A microarray-based protocol for monitoring the growth of yeast overexpression strains. *Nat. Protoc.* 2006; 1:569–576. [PubMed: 17406283]
60. Pierce SE, Davis RW, Nislow C, Giaever G. Genome-wide analysis of barcoded *Saccharomyces cerevisiae* gene-deletion mutants in pooled cultures. *Nat. Protoc.* 2007; 2:2958–2974. [PubMed: 18007632]

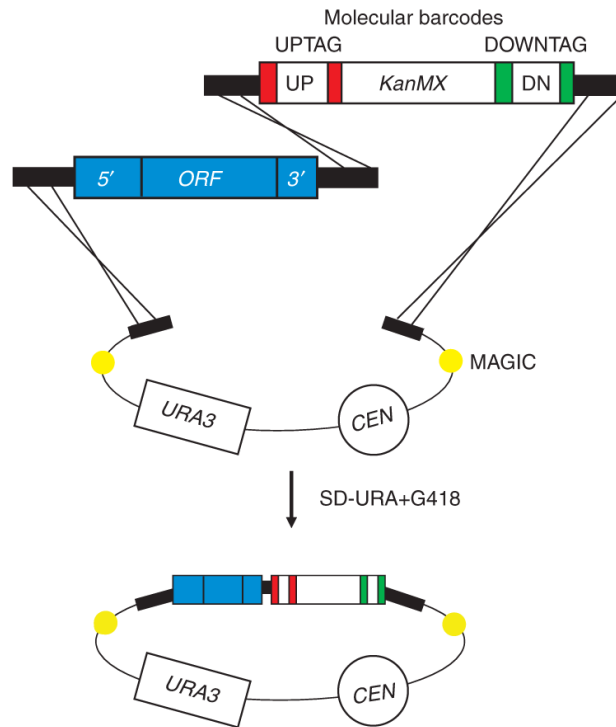


**Figure 1.**

Construction of the MoBY-ORF library by homologous recombination in yeast. Yeast cells are co-transformed with a PCR product encoding an ORF, a *KanMX* cassette, which confers G418/kanamycin resistance, and an *XhoI*-linearized vector that carries a selectable marker (*URA3*) and a yeast centromere sequence (CEN). Transformants are grown on synthetic medium that selects for recombinant plasmids. The *KanMX* cassette is flanked by two different molecular barcodes, labeled UPTAG and DOWNTAG, each of which are flanked by common primer sites, indicated in red and green. The *KanMX* barcode cassette for each gene was amplified from the corresponding deletion mutant for that gene. The vector backbone was designed to be compatible with the MAGIC system for manipulating plasmid inserts by homologous recombination in *Escherichia coli*. Filled yellow circles represent MAGIC recombination sites flanking the MoBY-ORF inserts.

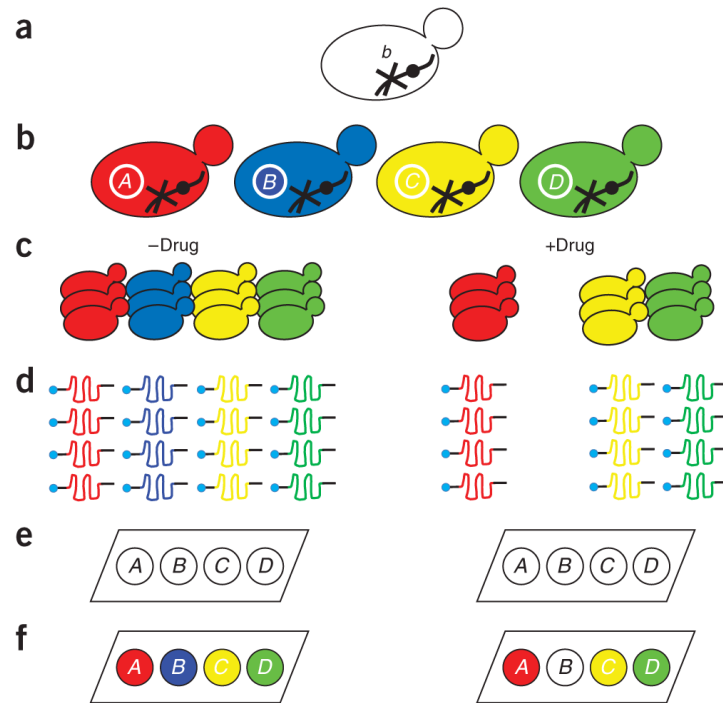


**Figure 2.** Identifying a recessive spontaneous drug-resistant mutant by MoBY-ORF complementation cloning. **(a)** Isolate a drug-resistant mutant. A chromosomal mutation in gene *B* leads to a drug-resistant allele (designated *b*). **(b)** Transform mutant with the MoBY-ORF library. In the example, plasmids carry wild-type copies of genes *A*, *B*, *C* and *D*. **(c)** Grow the pool of transformants in the absence and presence of a drug. The wild-type *B* allele complements the drug-resistant allele, causing the transformant that received *B* to be depleted from the pool with drug. **(d)** Extract plasmid DNA, PCR amplify and fluorescently label the barcode sequences. **(e)** Hybridize labeled barcode DNA to an Affymetrix TAG4 microarray. **(f)** Identify the transformant most depleted in the drug treated pool, in this case *B*.



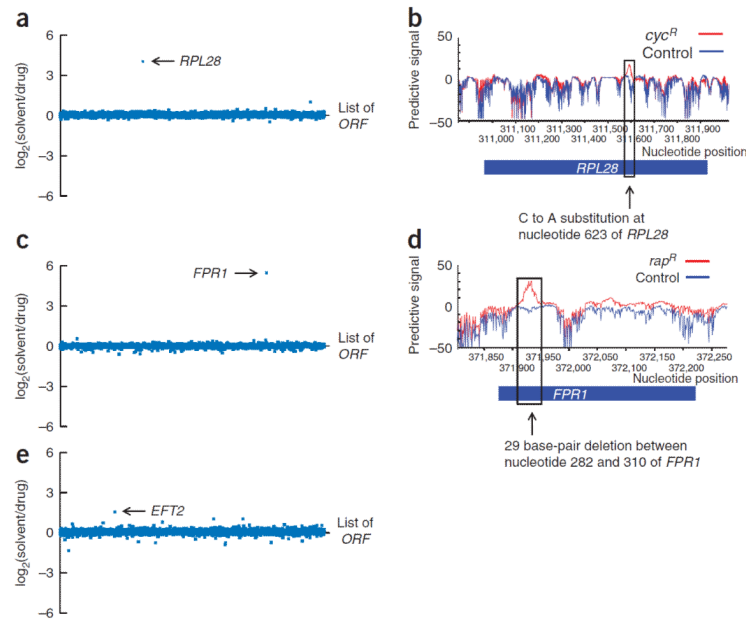


**Figure 3.**

Mapping a drug-resistant mutant by MoBY-ORF complementation cloning and yeast tiling microarrays. **(a)** Barcode depletion plot showing the relative levels of all MoBY-ORF plasmids in library-transformed, cycloheximide-resistant mutants (*cyc<sup>R</sup>*) grown in cyclohexamide (1  $\mu$ g/ml). Each point represents the relative abundance of a single plasmid in the untreated compared to drug-treated growth cultures (as measured by the y-axis ratio). An average value of the ratio of two independent experiments is shown. *RPL28* (*YGL103W*) was the ORF most depleted in the drug-treated pool. **(b)** Polymorphism prediction at the *RPL28* locus in *cyc<sup>R</sup>* mutant by whole-genome YTM analysis. Red and blue lines trace the log of the predictive signal (the likelihood ratio) for the presence of a SNP within the *RPL28* locus on chromosome VII. Direct sequencing identified a single-nucleotide substitution at nucleotide 623 of *RPL28*. **(c)** Barcode depletion plot for the rapamycin-resistant (*rap<sup>R</sup>*) mutant grown in the presence of rapamycin (5  $\mu$ g/ml). *FPR1* (*YNLI35C*) was the most depleted ORF. **(d)** Polymorphism prediction at the *FPR1* locus in *rap<sup>R</sup>* by whole-genome YTM. Direct sequencing identified a 29 base-pair deletion from nucleotide 282 to 310 of *FPR1*. **(e)** Barcode depletion plot for the sordarin-resistant (*sor<sup>R</sup>*) mutant grown in the presence of sordarin (50  $\mu$ g/ml). *EFT2* (*YDR385W*) was the most depleted ORF.

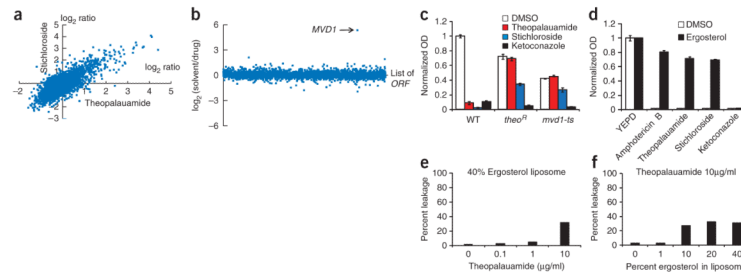


**Figure 4.**

MOA analysis of theopalauamide and stichloroside. **(a)** Correlation plot of chemical-genetic profiles of theopalauamide and stichloroside (correlation coefficient ( $R$ ) = 0.859). Points on the plot correspond to the log<sub>2</sub> ratio of control/drug-treated signal for each strain of ~5,000 viable haploid yeast deletion mutants (data are from ref. 9). **(b)** Barcode depletion plot for the theopalauamide- and stichloroside-resistant (*theo<sup>R</sup>*) mutant grown in medium containing theopalauamide (2 μg/ml). *MVD1* was the most depleted ORF. **(c)** Genetic evidence that theopalauamide and stichloroside do not inhibit Mvd1p. Growth after 16 h at 30 °C of a temperature-sensitive mutant of *MVD1* (*mvd1-ts*) and wild-type (WT) control in cultures containing theopalauamide (2.5 μg/ml), stichloroside (5 μg/ml), or ketoconazole (10 μg/ml). Bars show the means of three independent experiments. Error bars indicate s.d. **(d)** Ergosterol rescues the toxicity of theopalauamide and stichloroside. Growth after 16 h at 30 °C of WT cells in the presence of ergosterol (100 μg/ml) and either amphotericin B (10 μg/ml), theopalauamide (2 μg/ml), stichloroside (5 μg/ml), or ketoconazole (10 μg/ml). Number of replicates and error bars are as in **(c)**. **(e,f)** Theopalauamide permeabilizes liposomes containing ergosterol. Leakage of calcein, a fluorescent marker, from phosphatidylcholine liposomes containing ergosterol (40% in **(e)**, or a range of concentrations in **(f)**) after exposure to theopalauamide (a range of concentrations in **(e)**, or 10 μg/ml in **(f)**). Leakage was quantified relative to 100% calcein release from liposomes exposed to Triton-X 100. Bars show the averages of the two highly correlated replicates (Supplementary Fig. 6a,b).

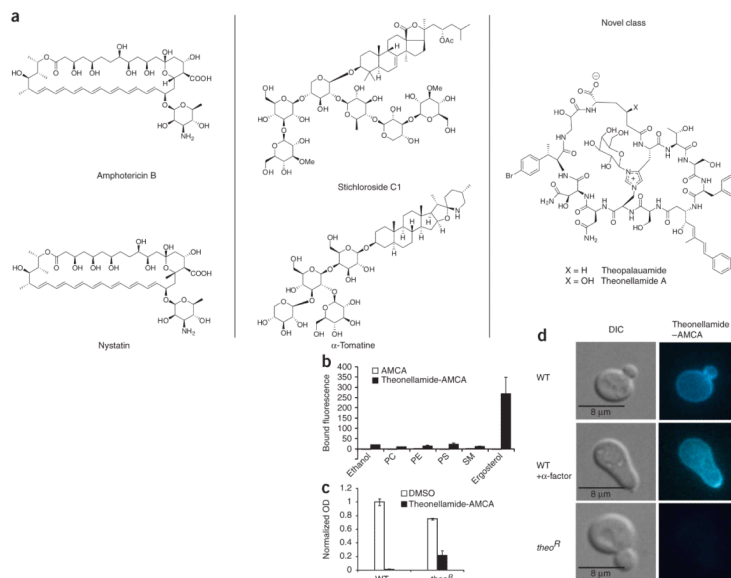


**Figure 5.** Theopalauamide and theonellamide represent a novel class of sterol-binding compound. **(a)** Amphotericin and nystatin belong to the polyene class of sterol-binding compound. Stichloroside belongs the saponin class, which includes  $\alpha$ -tomatine. Theopalauamide and theonellamide A represent a novel class of sterol-binding compound based on their unusual bicyclic structure bridged by a histidinoalanine residue. **(b)** *In vitro* binding of fluorescently labeled theonellamide A (theonellamide-AMCA) to ergosterol. Bars show the means of three independent experiments. PC, phosphatidylcholine; PE, phosphatidylethanol; PS, phosphatidylserine; SM, sphingomyelin. Error bars indicate s.d. **(c)** The theopalauamide/stichloroside-resistant (*theo<sup>R</sup>*) mutant is resistant to theonellamide (12.5  $\mu$ g/ml after 16 h of growth at 30  $^{\circ}$ C). Bars show the means of three independent experiments. Error bars indicate s.d. **(d)** Localization of theonellamide visualized by fluorescent microscopy. Cells were grown to mid-log phase.